

Article

Not peer-reviewed version

Selection of the Value of Power Distance Exponent for Mapping with the Inverse Distance Weighting Method - Application in Subsurface Porosity Mapping, Northern Croatia Neogene

[Uroš Barudžija](#)*, [Josip Ivšinić](#), [Tomislav Malvić](#)*

Posted Date: 26 April 2024

doi: 10.20944/preprints202404.1694.v1

Keywords: Inverse Distance Weighting (IDW Power distance exponent (p)); Neogene; Croatia; sandstone



Preprints.org is a free multidiscipline platform providing preprint service that is dedicated to making early versions of research outputs permanently available and citable. Preprints posted at Preprints.org appear in Web of Science, Crossref, Google Scholar, Scilit, Europe PMC.

Copyright: This is an open access article distributed under the Creative Commons Attribution License which permits unrestricted use, distribution, and reproduction in any medium, provided the original work is properly cited.

Article

Selection of the Value of Power Distance Exponent for Mapping with the Inverse Distance Weighting Method - Application in Subsurface Porosity Mapping, Northern Croatia Neogene

Uroš Barudžija ^{1,*}, Josip Ivšinović ² and Tomislav Malvić ^{1,*}

¹ Faculty of Mining, Geology and Petroleum Engineering, University of Zagreb, Pierottijeva 6, HR-10000 Zagreb, Croatia

² The 1st Catholic Elementary School in the City of Zagreb, Ivanićgradska 41A, HR-10000 Zagreb, Croatia; josip.ivsinovic@skole.hr

* Correspondence: uros.barudzija@rgn.unizg.hr (U.B.); tomlav.malvic@rgn.unizg.hr (T.M.)

Abstract: The correct selection of the value of p is a complex and iterative procedure that requires experience in the interpretation of the obtained interpolated maps. Inverse Distance Weighting is a method applied to the porosities of the K and L hydrocarbon reservoirs, discovered in the Neogene (Lower Pontian) subsurface sandstones in the northern Croatia (Pannonian Basin System). They represent small and large data samples. Also a standard statistical analysis of the data was made, followed by the qualitative-quantitative analysis of the maps, based on the selection of different values of the power distance exponent (p -value) for the K and L reservoirs maps. According to the qualitative analysis, for a small data set, p -value could be set on 1 or 2 giving the most optimal result, while for a large data set, a p value of 3 and 4 could be applied. By quantitative analysis, for the case of small data $p=2$ is recommended, resulting in a root mean square error value of 0.03458, a mean absolute error of 0.02013 and a median absolute deviation of 0.00546. Oppositely, a p -value of 3 and 4 is selected as appropriate for a large data set, with root mean square errors of 0.02435 and 0.02437, mean square errors of 0.01582 and 0.01509 and median absolute deviations 0.00896 and 0.00444. Eventually for a small data set, it is recommended to use a p -value of 2, and for a large data set, a p -value of 3 or 4.

Keywords: inverse distance weighting (IDW power distance exponent (p)); Neogene; Croatia; sandstone

1. Introduction

Inverse Distance Weighting (IDW) is an interpolation method that is widely used in geosciences. The method is applied to small and large input data sets. Various authors have applied IDW during different mappings of variables: mapping the distribution of a nickel deposit [1], geomorphology [2], estimated copper, molybdenum, gold and silver with respect to lithochemical data in the Kahang porphyry deposit in Central Iran [3], modeling of ionospheric time delay [4], spatial distribution maps of groundwater [5], spatial distribution of groundwater pollution maps [6], mapping of gold deposits based on drilled shallow wells [7], soil salinity mapping in the Mirzaabad District, Syrdarya Province [8], and the estimation of tin resources [9]. The estimated value of the IDW variable is calculated using the following formula: [10–12]:

$$z_{IDW} = \frac{\frac{z_1}{d_1^p} + \frac{z_2}{d_2^p} + \dots + \frac{z_n}{d_n^p}}{\frac{1}{d_1^p} + \frac{1}{d_2^p} + \dots + \frac{1}{d_n^p}} \quad (1)$$

where:

Z_{IDW} estimated value,

$d_1 \dots d_n$ distance between estimated value and known value 1...n,

p power distance exponent,
 $Z_1 \dots Z_n$ known values at locations $1 \dots n$.

The mapping results are greatly influenced by the power distance exponent (p), this is clear because it represents the exponent of a value that is inversely reciprocal to the known "hard" data, as can be seen from formula 1. This is why it is important to choose p correctly so that the obtained interpolated maps are usable and mathematically based. Both the size (small or large) and the nature of the input data set should be considered when choosing p . The wrong selection of p can lead to asymmetry in the resulting interpolation maps, which should be avoided. In this paper, the selection of p will be analyzed considering the quantitative (sample size, cross-validation) and qualitative (visual inspection and interpretation) aspects of the obtained interpolation maps.

2. Materials and Methods

For the analysis of the value of p , it is necessary to take into account the material and applied methods. The material data are contained in the values of the porosity of the reservoirs K and L. In addition to the previously described IDW, the coefficient of interquartile deviation, root mean square error, mean absolute error and median absolute deviation calculations were applied for analysis.

2.1. Coefficient of Interquartile Deviation

Coefficient of interquartile deviation (V_Q) is a measure of incomplete dispersion of a data set, and is defined as [13,14]:

$$V_Q = \frac{Q_3 - Q_1}{Q_1 + Q_3} \quad (2)$$

where:

V_Q coefficient of interquartile deviation,
 Q_1 the value of the lower (first) quartile of the sample,
 Q_3 the value of the upper (third) quartile of the sample.

The value of the coefficient is between 0 and 1, the condition for its application is that all input data are positive values (>0). The dispersion of the data is smaller the closer V_Q is to 0, and relatively larger the closer V_Q is to 1.

2.2. Root Mean Square Error (RMSE)

Cross-validation is a numerical value obtained as the difference of the square of the measured and estimated data values. Mean square error is calculated according to [15,16]:

$$MSE = \frac{1}{n} \sum_{i=1}^n (SV - P)_i^2 \quad (3)$$

where:

MSE - Mean Square Error value,
 n - number of known values,
 SV - measured value of point „ i “,
 P - estimated value of point „ i “,
 i - i^{th} point.

It quantitatively expresses the quality of the interpolation map, the lower the RMSE value, the higher the acceptability of the interpolated map. During the interpolation process while changing various parameters, RMSE is a corrective for interpolation maps because it reduces the space for gross errors. Root Mean Square Error value is calculated according to [17,18]:

$$RMSE = \sqrt{MSE} \quad (4)$$

where:

RMSE - Root Mean Square Error value,
MSE - Mean Square Error value.

RMSE due to the root function of the error itself means that larger errors will contribute less in absolute terms. This is very important when analyzing a large input data set.

2.3. Mean Absolute Error (MAE)

Mean Absolute Error is a measure of error calculated as the difference between the measured and estimated sample values. The formula for calculating MAE is [19,20]:

$$MAE = \frac{1}{n} \sum_{i=1}^n |SV - P|_i \quad (5)$$

where:

MAE - Mean Absolute Error,

n - number of known values,

SV - measured value of point „i“,

P - estimated value of point „i“,

i - ith point.

As can be seen from expression 5, the MAE represents a comparison between the "firm" data and the estimated data. The MAE method is sensitive to extreme values within the input data set.

2.4. Median Absolute Deviation (MAD)

Median absolute deviation is the median value of the difference between the estimated value and the value of the "solid" data. MAD is calculated according to the following equation [21,22]:

$$MAD = median(|SV - P|_i) \quad (6)$$

where:

MAD- Median Absolute Deviation,

SV - measured value of point „i“,

P - estimated value of point „i“,

i - ith point.

3. Geographic Location, Geological Settings and Raw Data of Analysed Reservoirs

Research fields "A" and "B" are located within the Sava Depression, in the Croatian part of the Pannonian Basin System (CPBS) (see **Figure 1**). Sediments filling the Sava Depression started already in Early Neogene (Otnangian), and in this study Lower Pontian reservoir rocks (reservoirs K and L) belonging to the Kloštar-Ivančić Formation are analyzed (see geological column in **Figure 1**). These are mainly well-sorted arenitic sandstones, becoming fine-grained and loose toward the top of the Široko Polje Formation, and intercalated with marl intervals. Reservoir rocks are well-lithified sandstones, with an average thickness of 20-150 m. Isolator rocks are gray to gray-brown marls, moderately lithified, appearing in 30-150 m thick intervals between sandstones.

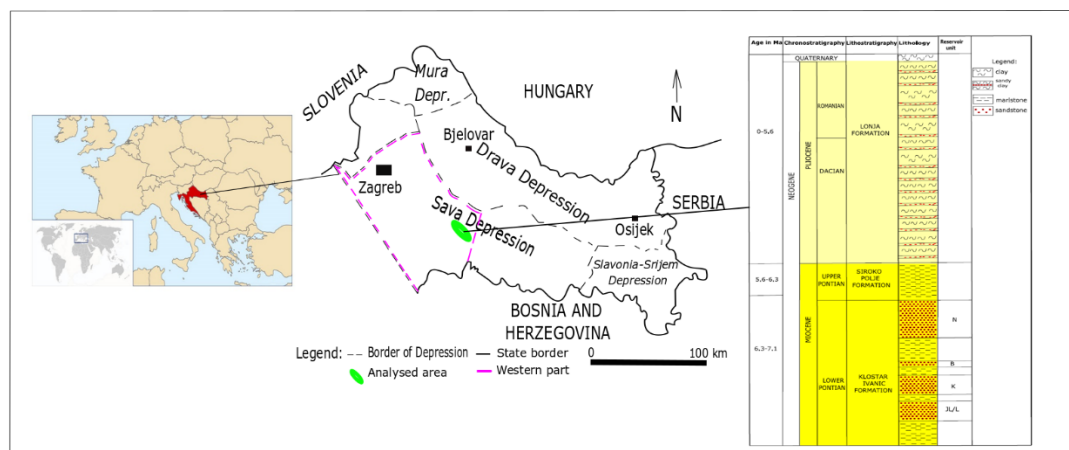


Figure 1. Geographical position and geological column of the research fields A and B within the Sava Depression, modified after [23,24].

The Lower Pontian sediments (also known informally by their older name Abichi deposits, after characteristic fossil shell *Paradacna abichi*) extended across the entire Sava Depression, but in the most western part can be represented with the Kloštar-Ivanić Marls (as lateral equivalent of the Kloštar-Ivanić Formation) or locally as the Brezine or Graberje Marl. The analysed sandstones (as part of the Poljana Sandstones) are the result of periodically activated turbidites and are deposited in the deepest part of the depression. The rest had been filled with marls, occasionally silty ones.

The most important petrophysical parameter during reservoir analysis is porosity. Data on the porosity of the deposits K and L were obtained by analyzing cores from a well or by interpreting logging diagrams. The porosity value for the K reservoir was obtained from 19 wells, while for the L reservoir it was obtained from 25 wells, and they are considered "solid" data, i.e. the original data during various analyses. Basic statistical data on the porosity of the reservoirs K and L are shown in **Table 1**. It is obvious that the quality and resolution of the measuring devices and the transformation of indirect signals into values had significant limitations, especially in the reservoir K, where numerous wells have the same average porosity value for sandstone. However, it is a common limitation that must be overridden using the most appropriate interpolation algorithm, and handled with the same values as some kind of "clusters", even if they are not located in their own neighborhood.

Table 1. Porosity data for reservoirs K and L [25].

Reservoir K				
Well	X	Y	Porosity (part of units)	Age
J-101	6421096	5028877	0.217	Lower Pontian
J-120	6420658	5029068	0.272	Lower Pontian
J-161	6420957	5028870	0.217	Lower Pontian
J-162	6421034	5028593	0.217	Lower Pontian
J-167	6420529	5028674	0.217	Lower Pontian
J-168	6420699	5028475	0.315	Lower Pontian
J-169	6420724	5028825	0.217	Lower Pontian
J-170	6420349	5028926	0.223	Lower Pontian
J-174	6421298	5028863	0.217	Lower Pontian
J-175	6420475	5029136	0.223	Lower Pontian
J-158	6420303	5028910	0.223	Lower Pontian
J-171	6420576	5028970	0.223	Lower Pontian
J-172	6420928	5029147	0.223	Lower Pontian
J-102	6421208	5028926	0.217	Lower Pontian
J-148	6421126	5028437	0.217	Lower Pontian
J-149	6420959	5028501	0.217	Lower Pontian
J-166	6420771	5028650	0.217	Lower Pontian
J-25	6420546	5028460	0.315	Lower Pontian
J-173	6420539	5028382	0.217	Lower Pontian
Reservoir L				
Well	X	Y	Porosity (part of units)	Age
L-111a	6417748	5027750	0.239	Lower Pontian
L-131a	6416847	5028084	0.156	Lower Pontian
L-136a	6416153	5028515	0.145	Lower Pontian
L-140	6415085	5028332	0.192	Lower Pontian
L-142	6415019	5028519	0.186	Lower Pontian
L-32	6416755	5028208	0.239	Lower Pontian
L-155	6416967	5028205	0.156	Lower Pontian
L-156	6415912	5028018	0.206	Lower Pontian
L-160	6416410	5028203	0.197	Lower Pontian
L-161	6416946	5028415	0.156	Lower Pontian
L-27	6416655	5028086	0.197	Lower Pontian
L-153	6417390	5027720	0.239	Lower Pontian
L-33a	6415763	5028687	0.214	Lower Pontian

L-33b	6415763	5028687	0.214	Lower Pontian
L-37	6415834	5028477	0.214	Lower Pontian
L-4a	6415435	5028754	0.214	Lower Pontian
L-5	6417200	5027939	0.239	Lower Pontian
L-57	6415946	5028104	0.206	Lower Pontian
L-62	6416091	5028355	0.206	Lower Pontian
L-65a	6415235	5028590	0.214	Lower Pontian
L-66	6415579	5028512	0.214	Lower Pontian
L-68	6415315	5028206	0.214	Lower Pontian
L-140	6414912	5028679	0.192	Lower Pontian
L-79	6414821	5028402	0.195	Lower Pontian
L-87alfa	6416347	5028297	0.197	Lower Pontian

4. Results and discussion

The choice of reservoir was made considering the size of the input data set. The size of the input data set is taken according to the authors [26], according to which the reservoir K belongs to a small data set, while the reservoir L belongs to a large data set. The values of the coefficient of interquartile deviation for the K and L reservoirs are presented in **Table 2**.

Table 2. Values of the coefficient of interquartile deviation for the K and L reservoirs.

Reservoir	Q1	Q3	V _Q
K	0.217	0.223	0.013
L	0.192	0.214	0.054

According to **Table 2**, the V_Q value for the K reservoir is 0.013, while for the L reservoir it is 0.054. According to these values, the porosity of these reservoirs is significantly dispersed. This was to be expected due to the nature of the input data and the method of obtaining it. Due to the high economic cost of obtaining data, the input data set is in most cases very dispersed. Precisely because of the large depressiveness of the data, the IDW method was applied for mapping the reservoirs K and L.

4.1. Qualitative Analysis of Maps

A qualitative analysis of interpolated maps implies a visual inspection of the map and the existence of the following visual mapping results: bulls-eye (circular), butterfly (ellipsoidal) and mosaic [27]. During the visual analysis of the maps, maps with a value of $p=0$ were not analyzed, because according to equation 1, in that case the solution of the equation would be same. The results of the mapping of reservoirs K and L using the IDW method for p values of 1,2,3 and 4 are shown in **Figures 2** and **3**.

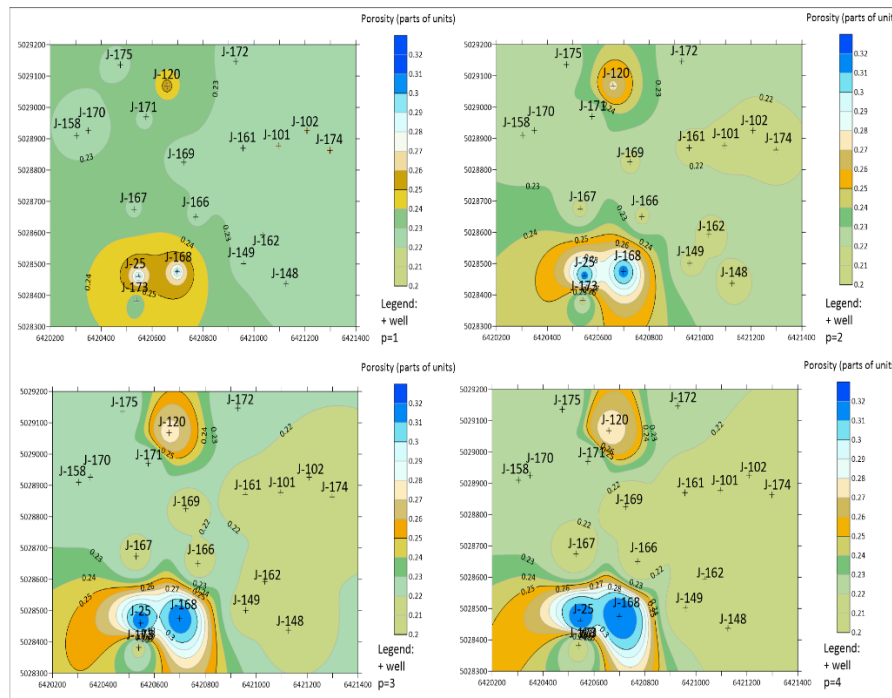


Figure 2. Maps of the porosity of the K reservoir obtained by the IDW method for values of $p=1,2,3,4$.

In the case of reservoir K (see **Figure 2**), with an increasing value of p , a pronounced bulls-eye effect ($p=1$, $p=2$) and butterfly effect ($p=3$, $p=4$) appears. At higher values, such as J-25, J-168, etc. regardless of the change in the value of p , the effect was not removed, but the changes were detected as a pronounced bulls-eye effect into a butterfly effect. With an increase in the value of p , there was no mosaic effect, which is positive. The transition zones are different in all cases of a change of p , the clearest transition zone is seen in the case of $p=2$ and does not have such a pronounced asymmetric value change, as in other cases. Also, with a p value of 2, it can be applied to reduce the number of bulls-eyes to only extreme values of the input data. In cases where bulls-eye and butterfly effects are expressed on the maps, from a visual point of view, interpolated maps with a bulls-eye effect are preferred. With the bulls-eye effect, the value is evenly distributed around the point data, while with the butterfly effect, there is an ellipsoidal surface around the point data, which due to the appearance can encompass space, which is not realistic. Therefore, on the example of the interpolated map obtained in **Figure 2**, i.e. in the case of a small data set, the value of p is 1 and 2 when using the IDW method.

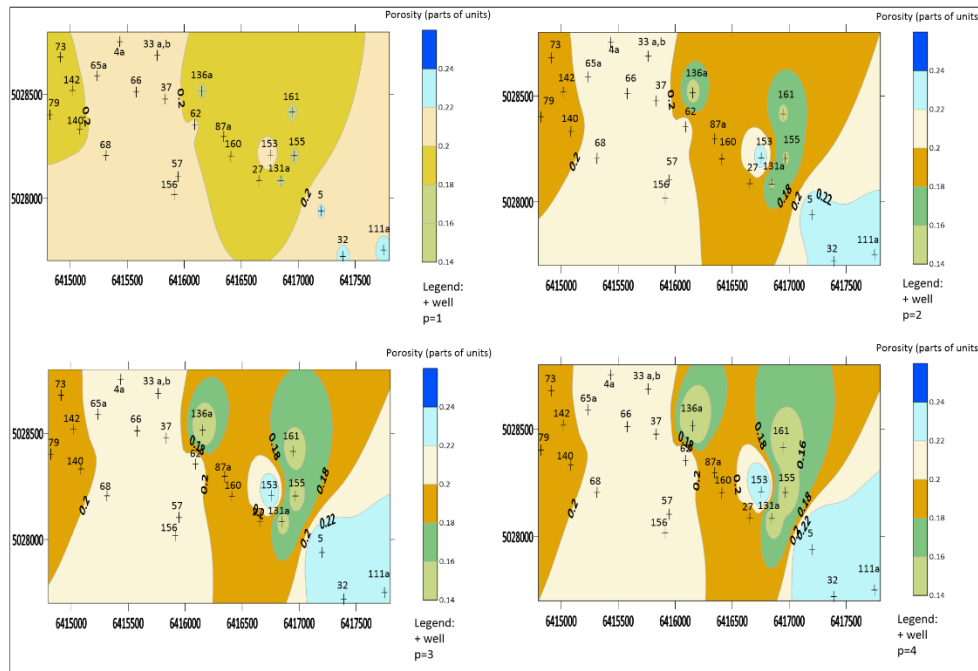


Figure 3. Maps of the porosity of the L reservoir obtained by the IDW method for values of $p=1,2,3,4$.

The porosity map of the reservoir L (see **Figure 3**) for all cases of p values have a pronounced butterfly effect. As the value of p increases in this case, the bulls-eye and mosaic effect are not present, which is evident from the obtained interpolation map. The reason for this is that it is a large data set, because the input data set is sufficient to perform a satisfactory interpolation in the given area. The transition area between different input data values is clearer when interpolating with p values of 3 and 4. For p values of 3 and 4, it is very clear that the reservoir L is tectonically very clearly divided and the stability of transition zones is conditioned by the values of individual data with neighboring ones, which can be seen in the eastern parts of the interpolated maps as a rather asymmetric area of porosity values. Considering the transition zones and the inclusion of input data in the interpolated maps, for a large data set, the recommendation from the visual inspection of the maps is to use p values of 3 and 4 when applying the IDW method.

4.2. Quantitative Analysis of Maps

The quantitative analysis is expressed by the numerical value of RMSE, MAE and MAD, the results of which are shown in **Table 3** for the K and L reservoirs.

Table 3. RMSE, MAE and MAD value for different values of p for the K and L reservoirs.

Reservoir	p	RMSE	MAE	MAD
K	1	0.03228	0.01700	0.00360
	2	0.03458	0.02013	0.00546
	3	0.03677	0.02196	0.00383
	4	0.03780	0.02276	0.00667
	5	0.03839	0.02319	0.00734
L	1	0.02632	0.01924	0.00869
	2	0.02505	0.01735	0.01012
	3	0.02435	0.01582	0.00896
	4	0.02437	0.01509	0.00444
	5	0.02470	0.01490	0.00343

The values of RMSE and MAE for the reservoir K increase as the value of the coefficient p increases, while the value of MAD varies. The RMSE values are 0.00104-0.00155, and the values of MAE are 0.01700-0.02319, which shows continuous but almost linear growth. The MAD value is not linear and takes on values 0.00360-0.00734. According to the RMSE, MAE and MAD values, the smallest value of the interpolated porosity map of the reservoir K with p values of 1 and 2. Unlike reservoir K, the RMSE, MAE and MAD values for reservoir L are not in a linear relationship. RMSE values are 0.0263-0.02470, MAE values are 0.01924-0.01490, and MAD values are 0.00869-0.00343. As can be seen from **Table 3**, for a value of p of 1, it has the highest value, while for values of p of 3 and 4, it has the lowest value for the interpolated maps of the porosity of the reservoir L. According to the quantitative methods and the RMSE, MAE and MAD values, for a small sample, the optimal value of p is 1 and 2, while for a large sample, the optimal value of p is 3 and 4.

4.3. Qualitative-Quantitative Approach in Selection of p -Value

Most of the authors who analyzed the p value in the IDW method took a data set that belongs to a large data set. Moreover, IDW is one of the most applied interpolation methods overall in many sciences that deal with spatial data, e.g. in mining [28] or soil mapping for military application [29]. However, the selection of p -value as standard for any scientific field is a very hard, if not impossible task, and often depends not only on discipline, but also on the geographical location of data. Such a geographically locked analysis is presented here as an example of subsurface geological mapping in the northern Croatia Neogene sandstones, and geological background defined what is considered as "small" and "large" data sets (in some other disciplines and locations, such definition could be totally different).

Both data sets had been considered for a comprehensive p -value analysis, including both qualitative and quantitative analyses, shown for the hydrocarbon reservoirs K and L of Lower Pontian age. Looking only of numerical values of the RMSE, MAE and MAD could lead to the conclusion that only the lowest values are criteria for the "best" p -value. Especially because Neogene northern Croatian sandstones are often of very heterogeneous porosity, including primary and secondary ones as the result of numerous events of compaction, relaxing, dissolutions and fracturing, as shown in **Figure 4**.

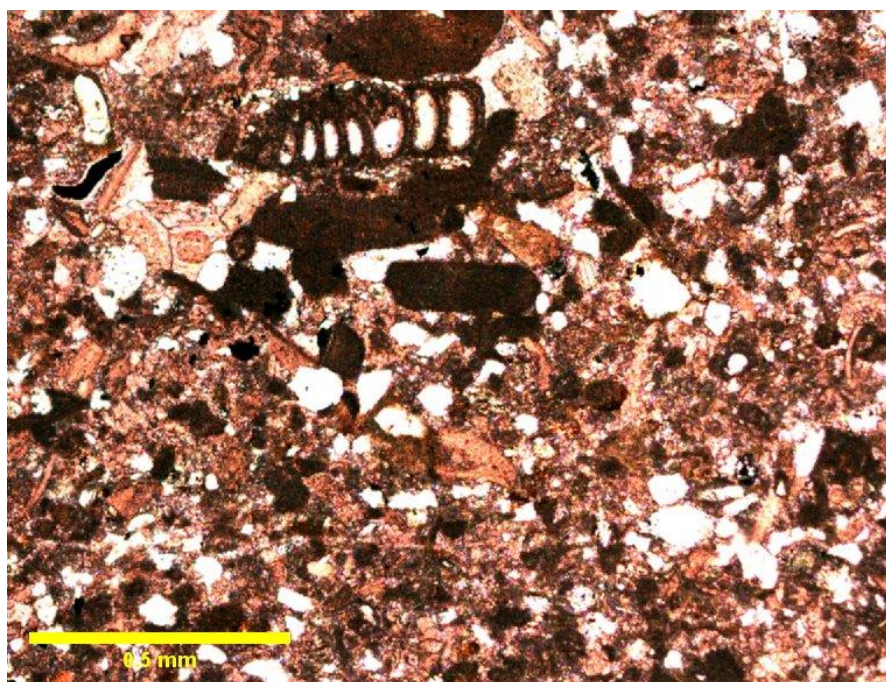


Figure 4. A photomicrograph of the typical Middle Miocene calcarenite from northern Croatia.

It is obligatory to also visually inspect the porosity maps and eliminate ones where some impossible subsurface shapes exist (like butterfly or too strong bulls-eye effects) or known faults with distorted isoporosity lines of continuity. Using both criteria, it is clear that for a small data set, the optimal p is 2, while for a large data set, the optimal value is 3 and 4. This is a recommendation for the application of the IDW method in the northern Croatia Lower Pontian sandstones porosity mapping, while it is definitely recommended for other sciences to analyze the input data set and perform a quantitative-qualitative analysis.

5. Conclusions

Data sets in geosciences are dispersed and in most cases are presented in the form of limited data sets. Two of them had been analysed for the porosity data of the K and L hydrocarbon reservoirs of the Neogene age in the northern Croatia. The main results of the qualitative-quantitative analysis are:

- For a small data set, it is recommended to use a p -value of 2, because in this case, the butterfly effect is eliminated, and the RMSE value of 0.00119, MAE value of 0.02103, and MAD value of 0.00546 are smaller with respect to larger p values.
- The p value of 3 and 4 is optimal in the case of a large data set, because the transition zones are clear and the input data set is included, and this is confirmed by the following values: RMSE (0.02435, 0.02437), MAE (0.01582, 0.01509) and MAD (0.00896, 0.00444).
- Data dispersion in the case of a small and large data set is present, but when changing the value of p , it gradually affects the obtained interpolation maps.
- The IDW method in both cases gave usable results and due to the similar lithologies in most of the Sava Depression (northern Croatia), it is recommended to apply the IDW method with p -values between 2-4, depending on the size of the analysed porosity data set.

Author Contributions: Conceptualization, J.I., U.B and T.M.; methodology J.I., U.B and T.M.; validation, J.I., U.B and T.M.; investigation, J.I.; writing—original draft preparation, J.I. and U.B.; writing—review and editing, J.I., U.B and T.M.; visualization, J.I. All authors have read and agreed to the published version of the manuscript.

Funding: Please add: This research received no external funding.

Data Availability Statement: Not applicable.

Acknowledgments: The authors thank the anonymous reviewers and editors for their generous and constructive comments that have improved this paper. This research was partially carried out in the projects “Mathematical researching in geology VIII” (led by T. Malvić).

Conflicts of Interest: The authors declare no conflicts of interest.

References

1. Bartier, P. M.; Keller, C. P. Multivariate interpolation to incorporate thematic surface data using inverse distance weighting (IDW). *Computers & Geosciences* **1996**, *22*(7), 795–799.
2. Gossel, W., Falkenhagen, M. Line-Geometry-Based Inverse Distance Weighted Interpolation (L-IDW): Geoscientific Case Studies. In Proceedings of the Mathematics of Planet Earth. Springer, Berlin, Germany, 08 October 2013. https://doi.org/10.1007/978-3-642-32408-6_74
3. Karami, R.; Afzal, P. Estimation of Elemental Distributions by Combining Artificial Neural Network and Inverse Distance Weighted (IDW) Based on Lithogeochemical Data in Kahang Porphyry Deposit, Central Iran. *Universal Journal of Geoscience* **2015**, *3*, 59 – 65. DOI: 10.13189/ujg.2015.030203.
4. Srinivas, V. S.; Sarma, A. D.; Achanta, H. K. Modeling of Ionospheric Time Delay Using Anisotropic IDW with Jackknife Technique. *IEEE Transactions on Geoscience and Remote Sensing* **2016**, *54*, 513-519. doi: 10.1109/TGRS.2015.2461017.
5. Mircovski, V.; Gicevski, B.; Dimov, G. Hydrochemical characteristics of the groundwaters in Prilep’s part of Pelagonia valley – Republic of Macedonia. *Rudarsko-geološko-Naftni Zbornik* **2018**, *33*, 111–119. <https://doi.org/10.17794/rgn.2018.3.11>
6. Maliqi, E.; Idrizi, B.; Penev, P. Compilation of groundwater monitoring maps for the Mitrovica region in Kosova. *Geoscience and Remote Sensing* **2019**, *2*, 41-55. DOI: <http://dx.doi.org/10.23977/geors.2019.21003>.
7. Liming S., Yingqi, W.; Hong C.; Jun, Y.; Jianzhang, X. Improved Fast Adaptive IDW Interpolation Algorithm based on the Borehole Data Sample Characteristic and Its Application. In Proceedings of the 3rd

- International Conference on Data Mining, Communications and Information Technology, Beijing, China, 24–26 May 2019. doi:10.1088/1742-6596/1284/1/012074
8. Pulatov, A.; Khamidov, A.; Akhmatov, D.; Pulatov, B.; Vasenev, V. Soil salinity mapping by different interpolation methods in Mirzaabad district, Syrdarya Province. In Proceedings of the International Scientific Conference Construction Mechanics, Hydraulics and Water Resources Engineering, Tashkent, Uzbekistan, 23-25 April 2020. doi:10.1088/1757-899X/883/1/012089
 9. Gonzales, R.; Rahardi, M. R. G.; Octova, A. Estimation of tin resources using Inverse distance weighted (IDW) and nearest neighbor point (NNP) methods in Bangka Tengah district, Bangka Belitung islands province. *Georest* **2023**, *2*, 1–7. <https://doi.org/10.57265/georest.v2i1.12>
 10. Achilleos, G.A. The Inverse Distance Weighted interpolation method and error propagation mechanism – creating a DEM from an analogue topographical map, *Journal of Spatial Science* **2011**, *56*, 283-304. <http://dx.doi.org/10.1080/14498596.2011.623348>
 11. Maleika, W. Inverse distance weighting method optimization in the process of digital terrain model creation based on data collected from a multibeam echosounder. *Appl Geomat* **2020**, *12*, 397–407. <https://doi.org/10.1007/s12518-020-00307-6>
 12. Liu, Z.; Zhang, Z.; Zhou, C.; Ming, W.; Du, Z. An Adaptive Inverse-Distance Weighting Interpolation Method Considering Spatial Differentiation in 3D Geological Modeling. *Geosciences* **2021**, *11*, 51. <https://doi.org/10.3390/geosciences11020051>
 13. Yadav, S.K.; Singh, S.; Gupta, R. Measures of Dispersion. In: *Biomedical Statistics*; Springer, Singapore, 2019; pp. 59-71. https://doi.org/10.1007/978-981-32-9294-9_8
 14. Botta-Dukát, Z. Quartile coefficient of variation is more robust than CV for traits calculated as a ratio. *Sci Rep* **2023**, *13*, 4671. <https://doi.org/10.1038/s41598-023-31711-8>
 15. Browne, M. W. Cross-Validation Methods. *Journal of Mathematical Psychology* **2000**, *44*(1), 108–132. doi:10.1006/jmps.1999.1279
 16. Rodríguez, J.D.; Martínez, A.P.; Lozano, J.A. Sensitivity Analysis of k-Fold Cross Validation in Prediction Error Estimation. *IEEE Transactions on Pattern Analysis and Machine Intelligence* **2010**, *32*, 569-575.
 17. Chai, T.; Draxler, R.R. (2014). Root mean square error (RMSE) or mean absolute error (MAE)?– Arguments against avoiding RMSE in the literature. *Geoscientific Model Development* **2014**, *7*, 1247-1250. doi: 10.5194/gmd-7-1247-2014.
 18. Čalasan, M.; Abdel Aleem, S. H. E.; Zobaa, A. F. On the root mean square error (RMSE) calculation for parameter estimation of photovoltaic models: A novel exact analytical solution based on Lambert W function. *Energy Conversion and Management* **2020**, *210*, 112716. doi:10.1016/j.enconman.2020.11271
 19. Willmott, C. J.; Kenji M. Advantages of the mean absolute error (MAE) over the root mean square error (RMSE) in assessing average model performance. *Climate Research* **2005**, *30*, 79-82.
 20. Hodson, T. O. Root-mean-square error (RMSE) or mean absolute error (MAE): when to use them or not. *Geoscientific Model Development* **2022**, *15*. <https://doi.org/10.5194/gmd-15-5481-2022>
 21. Pham-Gia, T.; Hung, T.L. The mean and median absolute deviations. *Mathematical and Computer Modelling* **2001**, *34*, 921-936. [https://doi.org/10.1016/S0895-7177\(01\)00109-1](https://doi.org/10.1016/S0895-7177(01)00109-1)
 22. Elamir, E. Mean Absolute Deviation about Median as a Tool of Explanatory Data Analysis. *International Journal of Recent Research and Applied Studies* **2012**, *11*, 517-523.
 23. Ivšinović, J.; Malvić, T. Application of the radial basis function interpolation method in selected reservoirs of the Croatian part of the Pannonian Basin System. *Mining of mineral deposits* **2020**, *14*, 37-42. doi:10.33271/mining14.03.037.
 24. Ivšinović, J.; Pimenta Dinis, M.A.; Malvić, T.; Pleše, D. (2021) Application of the bootstrap method in low-sampled Upper Miocene sandstone hydrocarbon reservoirs: a case study. *Energy Sources, Part A: Recovery, Utilization, and Environmental Effects* **2021**, *41* 1-15. DOI: 10.1080/15567036.2021.1883773
 25. Malvić, T.; Ivšinović, J.; Velić, J.; Rajić, R. Kriging with a Small Number of Data Points Supported by Jack-Knifing, a Case Study in the Sava Depression (Northern Croatia). *Geosciences* **2019**, *9*, 36. <https://doi.org/10.3390/geosciences9010036>
 26. Malvić, T.; Ivšinović, J.; Velić, J.; Rajić, R. Interpolation of Small Datasets in the Sandstone Hydrocarbon Reservoirs, Case Study of the Sava Depression, Croatia. *Geosciences* **2019**, *9*, 201. <https://doi.org/10.3390/geosciences9050201>
 27. Ivšinović, J.; Malvić, T. Comparison of mapping efficiency for small datasets using inverse distance weighting vs. moving average, Northern Croatia Miocene hydrocarbon reservoir. *Geologija* **2022**, *65*, 47–57. <https://doi.org/10.5474/geologija.2022.003>
 28. Rezaei, M., & Fallahi, S. (2023). Block model optimization and resource estimation of the Angouran Mine by transferring the exploratory data from the local coordinate system to the UTM. *Rudarsko-geološko-Naftni Zbornik*, *38*(3), 1–17. <https://doi.org/10.17794/rgn.2023.3.1>
 29. Heštera, H., Pahernik, M., Kovačević Zelić, B., & Maurić Maljković, M. (2023). The Unified Soil Classification System Mapping of the Pannonian Basin in Croatia using Multinomial Logistic Regression

and Inverse Distance Weighting Interpolation. *Rudarsko-geološko-Naftni Zbornik*, 38(3), 147–159.
<https://doi.org/10.17794/rgn.2023.3.12>.

Disclaimer/Publisher's Note: The statements, opinions and data contained in all publications are solely those of the individual author(s) and contributor(s) and not of MDPI and/or the editor(s). MDPI and/or the editor(s) disclaim responsibility for any injury to people or property resulting from any ideas, methods, instructions or products referred to in the content.